DOI: 10.1002/anie.200905339

Hybrid Composites

A Molecular Double Decker: Extending the Limits of Current Metal–Molecule Hybrid Structures**

Felix Eberle, Marc Saitner, Hans-Gerd Boyen, Jan Kucera, Axel Gross, Andriy Romanyuk, Peter Oelhafen, Marc D'Olieslaeger, Mila Manolova, and Dieter M. Kolb*

Since the first proposal[1] by Aviram and Ratner to use organic molecules as new building blocks for information technology, tremendous efforts have been spent to implement basic electronic units such as rectifiers or transistors.[2] To fabricate appropriate metal–molecule–metal hybrid structures, two strategies have been followed in recent years, resulting in either planar or sandwich arrangements of the involved materials.[3] In the planar design, nanolithography at its current technological limits is required to manufacture metal electrodes with gaps precisely corresponding to the length of the molecules involved (1–3 nm). In the sandwich design, counter electrodes need to be deposited on top of molecular layers without destroying the assembly by interdiffusion.[3,4] The successful metallization of self-assembled organic monolayers (SAMs) can reliably be achieved with only a few methods.[3] Among those, electrochemical techniques[5,6] proved to be quite powerful, as they allow variation of both the type of molecules and the metals involved.[5–9]

To increase the functionality of molecule-based nanoelectronic devices in the future, a significant increase in the complexity of their architecture might be required. As a vision, combinations of different molecular layers which can be electrically contacted by individual metal electrodes could serve as a new platform for this ambitious aim. Thus, it appears rather appealing to extend the sandwich design (one organic layer involved) to a molecular double decker (two separate organic layers) and, finally, to a molecular multilayer. Herein, we present theoretical and experimental evidence that a stable molecular double decker can be prepared, representing a proof-of-principle for the first step towards a 3D metal–molecule hybrid structure. The sample consists of a Au(111) single crystal as base electrode, a layer of 4-mercaptopyridine (Mpy) molecules forming the first SAM, a nearly closed Pd monolayer as a spacer, and a second Mpy SAM, which is metallized by a (sub-)monolayer of Pt atoms as the terminal electrode. We demonstrate that the Pd interlayer still reveals metallic properties despite the presence of two SAMs attached to it by chemical bonds. Such metallic interlayers might be useful as "intermediate electrodes" in future experiments, thus offering a new possibility to influence and control charge transport through metal–molecule hybrid structures.

To assess the stability of the suggested layer sequence at the microscopic level, structural optimization was performed from first principles within density functional theory (DFT). Moreover, these calculations allowed us to investigate the nature of the binding between the different constituents of the arrangement. Figure 1 illustrates the resulting structural model in which a $(\sqrt{3}\times\sqrt{3})R30°$ ($R30°$ = rotated by 30°) arrangement of the adsorbed organic layer is assumed, the stability of which at high Mpy coverages (1/3 molecule per Au atom) was previously confirmed theoretically.[10] Mpy molecules on a Au(111) surface are stabilized through chemical bonds between their sulfur head group and either one, two, or three surface gold atoms at the top, bridge, and hollow sites, respectively.[10]

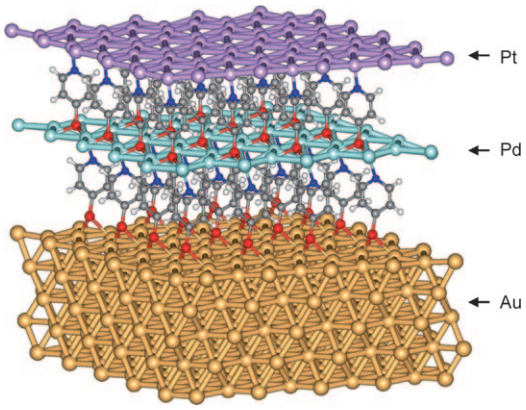

Figure 1. Side view of the computed DFT geometry for a stable Au/Mpy/Pd/Mpy/Pt double-decker structure. S red, N blue, C gray, H white.

[*] M. Saitner, Prof. H.-G. Boyen, Prof. M. D'Olieslaeger
Institute for Materials Research (IMO), Hasselt University
3590 Diepenbeek (Belgium)
E-mail: hansgerd.boyen@uhasselt.be
Prof. M. D'Olieslaeger
IMEC, division IMOMEC
3590 Diepenbeek (Belgium)
F. Eberle, Dr. M. Manolova, Prof. D. M. Kolb
Institut für Elektrochemie, Universität Ulm
89069 Ulm (Germany)
Dr. J. Kucera, Prof. A. Gross
Institut für Theoretische Chemie, Universität Ulm
89069 Ulm (Germany)
Dr. A. Romanyuk, Prof. P. Oelhafen
Departement Physik, Universität Basel
Klingelbergstrasse 82, 4056 Basel (Switzerland)

[**] Financial support from the Deutsche Forschungsgemeinschaft within SFB 569, the Belgium Odysseus and Interuniversity Attraction Pole programs, the Swiss National Science Foundation, and the NCCR "Nanoscale Science" is gratefully acknowledged. The authors also thank Dr. G. Kästle for fruitful discussions and J. Baccus for technical assistance.

With the sulfur head being bound to gold, the palladium adlayer interacts with the Mpy molecules through their nitrogen tail. In a first step, we addressed the bond between a bare Pd atom and the N atom of an isolated Mpy molecule on Au(111) within a 3×3 geometry corresponding to a Mpy coverage of 1/9 per Au atom. We found a Pd–N bond length of 0.203 nm and a binding energy of −1.47 eV that were basically independent of the particular Mpy adsorption site on Au. Interestingly, the geometry of the S–Au contact is only negligibly affected by formation of a Pd–N bond at the other side of the molecule. For the complete Pd monolayer on Mpy/Au within a $(\sqrt{3}\times\sqrt{3})R30°$ structure, there are three Pd atoms per Mpy molecule. According to the DFT calculations, only one out of three Pd atoms binds directly to the Mpy molecules on Au, thereby forming a one-fold coordinated bond of length 0.202 nm between N and Pd.

When the second molecular layer is added to the stack, the molecules bind to the underlying palladium monolayer through the sulfur head group at a three-fold-coordinated hollow site (S–Pd distances ca. 0.22 nm), whereas the nitrogen tail again forms a one-fold coordinate bond to the platinum adlayer (N–Pt distance ca. 0.20 nm) when completing the sample by its top electrode. As far as the orientation of the Mpy molecules between the metal layers is concerned, it is natural to assume that the sulfur atoms of the first SAM bind to Au and those of the second SAM to Pd because of the sequential assembly of the hybrid structure. This situation, however, could represent a metastable rather than a stable configuration if the stacking sequence Pd/S-SAM-N/Pt would energetically be less favorable than the sequence Pd/N-SAM-S/Pt. In the latter case, a reorientation of the molecules could be expected with time, making the sample thermodynamically unstable. Therefore, isolated single palladium and platinum layers sandwiching the SAM (organized in a $(\sqrt{3}\times\sqrt{3})R30°$ geometry) were simulated to find out the ground-state energies for both molecular orientations. To account for relaxation effects within the metal layers, we used interatomic distances within the layers of 0.263, 0.280, and 0.288 nm, spanning the range from the Pd–Pd to the Au–Au bulk distance. In all cases, the sequence Pd/S-SAM-N/Pt was found to be energetically more favorable, with an energy difference decreasing with increasing metal–metal distance (from −0.77 eV at 0.263 nm to −0.16 eV at 0.288 nm), thus indicating a good chance to experimentally assemble a stable molecular double decker according to the structural model illustrated in Figure 1.

All samples were prepared by means of a recently developed electrochemical approach,[5,7–9] which combines elements of currentless deposition and electrodeposition. Briefly, a first molecular layer is adsorbed on top of a Au(111) single crystal. In a following step, the complexation between Pd^{2+} ions and the ring nitrogen atom of the Mpy molecules is achieved by immersing the SAM-covered gold electrode for 15 min in a mixture of 0.1 mM $PdSO_4$ and 0.1 M H_2SO_4. Finally, by a subsequent potential scan in negative direction, the complexed metal ions are reduced to Pd^0 in a metal-ion-free electrolyte, thus allowing the Pd atoms to form strictly two-dimensional metal islands of monoatomic height on top of the SAM (Figure 2a). An island coverage of about 30% can be recognized. Assuming that one functional group can bind one metal ion,[5,7,8] this result is consistent with the supposition of a $(\sqrt{3}\times\sqrt{3})R30°$ structure for the SAM. To increase the coverage of metal atoms on top of the first SAM, the sample was immersed in the $PdSO_4$ solution two more times, immediately followed by the corresponding reduction step as described before. In this way, the Pd coverage could be raised to nearly a full monolayer (coverage greater than 95% as determined by STM), although the second Pd layer already started to grow (Figure 2b). In the next step, the sandwich was immersed once more into an Mpy solution for adsorption of the second SAM and another subsequent complexation step, this time with Pt^{2+} ions. Finally, after the reduction in a metal-ion-free electrolyte, Pt islands can be observed to form a top layer with a coverage of 30% (Figure 2c). As before, this value can be increased by repeating the basic cycle of our electrochemical approach (Figure 2d).

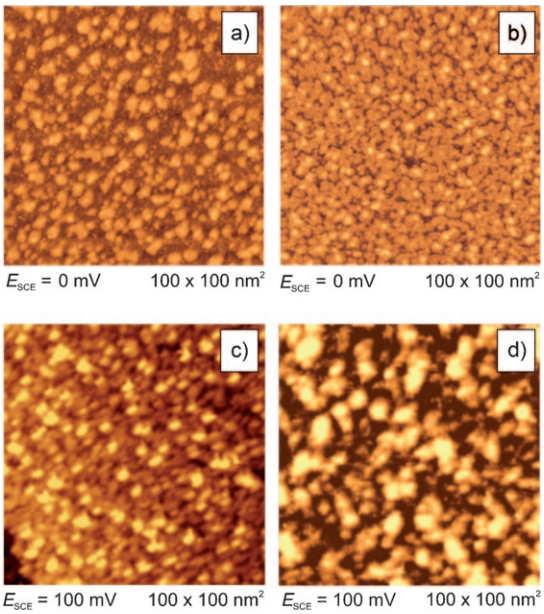

Figure 2. Morphology of the double-decker junction after different preparation steps. STM images were taken from the SAM on top of the Au single crystal a) after the deposition of 1/3 of a Pd monolayer and b) after the third complexation cycle followed by a reduction step, thus indicating the formation of a nearly closed Pd monolayer. c,d) Sample morphology after adding the second SAM on top of the Pd layer and subsequent metallization, with Pt islands at coverages of about 1/3 of a monolayer (c) and 2/3 of a monolayer (d).

Final evidence for the successful assembly of the desired structure comes from X-ray photoelectron spectroscopy (XPS). Spectra of element-specific core levels were acquired as a function of the emission angle α, thereby allowing variation of the surface sensitivity of the experiment. The results are summarized in Figure 3, which shows the ratios of the core-line intensities originating from the Au substrate and either the SAMs (Figure 3a), the Pd interlayer (Figure 3b), or the Pt top layer (Figure 3c) as a function of α (symbols); all data are normalized to the respective values found for emission in the normal direction ($\alpha=0°$). While going from normal incidence to nearly grazing incidence, the photoelectrons emitted from the Au substrate are found to be

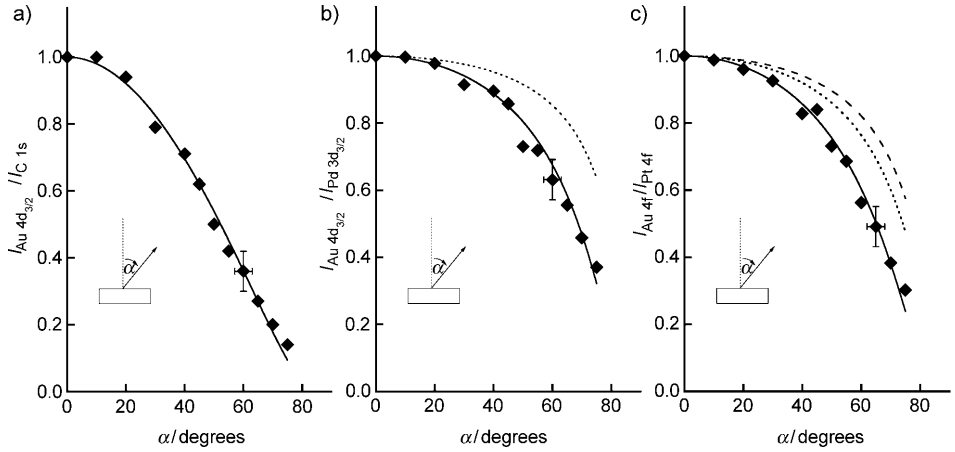

Figure 3. Angular dependence of the intensity ratios of the a) Au $4d_{3/2}$ vs. C 1s, b) Au $4d_{3/2}$ vs. Pd $3d_{3/2}$, and c) Au 4f vs. Pt 4f line intensities. Experimental data are represented by full symbols. Theoretical values assuming different layer sequences are shown as lines: simulation according to the model presented in Figure 1 (solid lines in a–c); Pd layer underneath the first molecular layer (dotted line in b); Pt layer on top of the Pd interlayer induced by Pt diffusion through the second SAM (dashed line in c); Pt diffusing through the second SAM forming an alloy with the Pd interlayer (dotted line in c).

strongly attenuated in all cases. This variation enables comparison with predictions obtained by assuming that each individual layer of the stack attenuates the intensity of photoelectrons escaping from any of the buried layers underneath (see the Experimental Section).

As a first step, the thickness of the organic layers can be derived from Figure 3a by fitting the double-decker model to the experimental results (solid line). In this way, a total thickness of 1.32 nm for the molecular contribution to the stack can be extracted (corresponding to a thickness of 0.66 nm for each individual SAM), which agrees well with previous work[5] and which indicates that the molecules most likely stand nearly vertically on their respective metallic supports, as assumed in Figure 1. As a second step, using a thickness of 0.66 nm for each SAM and the known coverages of the involved metal over- and interlayers, the dependence of the corresponding Au 4d/Pd 3d and Au 4f/Pt 4f intensity ratios on α can be predicted. The resulting data have been added to Figure 3b,c as solid lines and show good agreement between experiment and simulation. It is worth noting that different Au core levels were selected for comparison with the other metals involved (Au 4d vs. Pd 3d; Au 4f vs. Pt 4f) to guarantee nearly identical kinetic energies of the escaping photoelectrons. In this way, corrections of line intensities related to the transmission function of the energy analyzer can be avoided. Furthermore, Au 4f photoelectrons (Figure 3c), owing to their higher kinetic energies as compared to Au 4d photoelectrons, will be less damped while traveling through the different layers. As a consequence, similar angular dependencies for the Au 4d/Pd 3d and Au 4f/Pt 4f intensity ratios are obtained even though, at first sight, a stronger damping might be expected for the Au 4f/Pt 4f ratio resulting from the larger spacing between the Au support and the Pt top electrode.

To investigate deviations from the layer sequence illustrated in Figure 1, additional simulations were performed for various sample scenarios. Assuming, on the one hand, that the Pd layer diffuses through the first SAM towards the Au base electrode results in significant deviations from the measured data (Figure 3b, dotted curve). On the other hand, Pt atoms diffusing through the second SAM, thereby forming (most probably) a Pt–Pd intermixed layer, will result in an angular dependence as given by the dotted line in Figure 3c. Again, significant deviations from the measured values are obvious. Thus, angle-resolved XPS provides evidence for the successful electrochemical metallization of the contributing molecular layers without destruction of the assembly. The controlled intercalation of the Pd monolayer between two molecular layers is also supported by the observation of an additional chemical shift of the Pd 3d core lines towards higher binding energies after adding the second SAM (Figure 4a), reflecting the presence of chemical bonds at both metal–molecule interfaces. It is worth mentioning that although Au–S bonds are known to be oxidized over time, no significant contribution of sulfur atoms in higher oxidation states (S $2p_{3/2}$ 165–168 eV) could be detected, at least on the time scale of our experiments (weeks).

So far, the Pd monolayer only served as a support for the attachment of the second organic layer though Pd–S bonds. This situation raises the question as to what extent a single layer of metal atoms, sandwiched between two molecular layers, could also be used as an ultrathin intermediate electrode in future experiments. While a nearly closed Pd monolayer attached to a single Mpy SAM was found to be metallic,[11] nonmetallic behavior appears likely in the present case, as two molecular layers are interacting through chemical bonds at both sides of the metal layer. To address this important question, additional experiments were carried out to unravel the electronic structure of a Pd layer sandwiched between two Mpy SAMs. First, valence-band spectra were acquired after appropriate preparational steps (Au/Mpy and Au/Mpy/Pd/Mpy) applying ultraviolet photoelectron spectroscopy (UPS, 40.8 eV). By subtracting both spectra from each other and by taking into account a HOMO–LUMO gap of the molecules of at least 4 eV,[11] the electronic density of states of the Pd layer can be extracted within a binding energy range of 0–4 eV. The corresponding result is presented in Figure 4b (bottom curve), clearly revealing the metallic character of the interlayer by means of a nonvanishing intensity at the Fermi energy ($E_B = 0$).

To further test this important conclusion, the photoemission experiments were repeated using XPS (1486.6 eV), which enables strong suppression of the photoemission from

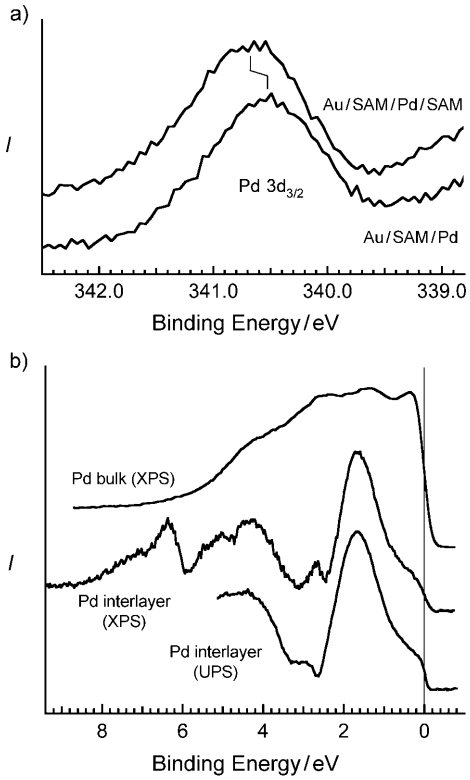

Figure 4. a) Pd $3d_{3/2}$ core-level spectra measured after the deposition of a Au/Mpy/Pd sandwich structure before (lower curve) and after (upper curve) the deposition of the second SAM on top of the Pd monolayer. b) Valence-band spectra of the Pd interlayer as determined from UPS (40.8 eV, bottom curve) and XPS (1486.6 eV, middle curve) in comparison with a Pd bulk reference sample (1486.6 eV, top curve).

the SAMs owing to significantly reduced photoionization cross sections for C 2p or N 2p, for example.[12] As before, a metallic behavior of the Pd interlayer can be recognized (middle curve) when taking into account the reduced energy resolution of XPS (full width at half maximum (FWHM) 0.30 eV) as compared to UPS (FWHM 0.03 eV). On the other hand, the comparison with the valence-band spectrum taken on a Pd bulk sample (top curve) also indicates a significantly reduced density of states at the Fermi level for the Pd interlayer. This change is accompanied by the appearance of several new features in the band shape, reflecting the chemical interaction between the Pd atoms and the two SAMs.

The deposition of a second SAM on top of a metallized first SAM representing the first step towards a metal–molecule double decker has been tried recently.[13] However, unequivocal proof by, for example, angle-resolved XPS using monochromatic X-rays to avoid radiation damage[14] has not been provided. On the other hand, the periodic complexation with one type of metal ions and the subsequent deposition of one type of molecular layer resulting in a step-by-step growth of multilayers has been demonstrated several times in the past.[15–20] In contrast, our approach has the potential to combine different types of molecular layers and different types of metallic interlayers into a single hybrid structure, thereby offering a new pathway to the design of new functional properties of metal–molecule assemblies.

In conclusion, we have shown that a stable metal–molecule double decker can be prepared and understood by combining electrochemical techniques, DFT simulations, and photoelectron spectroscopy. It is demonstrated that the metal interlayer still reveals metallic properties despite the presence of two SAMs attached to it from both sides. Thus, such metal interlayers might be useful as intermediate electrodes in forthcoming studies, thus offering another possibility to control charge transport through such metal–molecule hybrid structures.

Experimental Section

Photoelectron spectroscopy: Core-level spectra were acquired using $Al_{K\alpha}$ X-rays (1486.6 eV) as provided by two commercial photoemission systems (Fisons ESCALAB 210, Physical Electronics PHI 5600LS). In both cases, radiation damage to the SAMs induced by secondary electrons[21] could be avoided using monochromator systems. The binding-energy scale of both instruments was calibrated by means of independent Au reference samples (Au 4f: 84.0 eV).

The experimental intensity ratios were obtained by integrating the appropriate core line intensities using a Shirley type background.[22] The resulting data were compared with predictions, assuming that each individual layer attenuates the photoelectron intensities escaping from all layers underneath.[23,24] In our simulations, the following mean free path values were used depending on the material to be traveled through and the kinetic energy of the escaping photoelectrons: 1) 1.7 nm for Au 4d, Pd 3d, and C 1s photoelectrons traveling through another metal,[25,26] 2) 3.4 nm for Au 4d, Pd 3d, and C 1s photoelectrons traveling through either of the two SAMs,[27] 3) 1.8 nm for Au 4f and Pt 4f photoelectrons traveling through another metal,[25,26] and 4) 4.3 nm for Au 4f and Pt 4f photoelectrons traveling through either of the two SAMs.[27]

Computational details: The periodic DFT calculations were performed using the VASP code.[28] For the treatment of exchange–correlation effects, the Perdew–Becke–Ernzerhof (PBE) functional was employed.[29] The core electrons were treated by the projected augmented wave method,[30,31] and the electronic wave functions were expanded in a plane-wave basis set with an energy cutoff of 400 eV. The Au(111) substrate was described by a slab with a thickness of five layers.

Received: September 23, 2009
Published online: ■■ ■■, 2009

Keywords: density functional calculations · electrochemical deposition · molecular double decker · organic–inorganic hybrid composites · self-assembly

[1] A. Aviram, M. A. Ratner, *Chem. Phys. Lett.* **1974**, *29*, 277.
[2] *Introducing Molecular Electronics (Lecture Notes in Physics)* (Eds.: G. Cuniberti, G. Fagas, K. Richter), Springer, Berlin, **2005**.
[3] H. Haick, D. Cahen, *Prog. Surf. Sci.* **2008**, *83*, 217.
[4] C. Silien, N. A. Pradhan, W. Ho, P. A. Thiry, *Phys. Rev. B* **2004**, *69*, 115434.
[5] T. Baunach, V. Ivanova, D. M. Kolb, H.-G. Boyen, P. Ziemann, M. Büttner, P. Oelhafen, *Adv. Mater.* **2004**, *16*, 2024.
[6] I. Thom, G. Hähner, M. Buck, *Appl. Phys. Lett.* **2005**, *87*, 024101.
[7] M. Manolova, V. Ivanova, D. M. Kolb, H.-G. Boyen, P. Ziemann, M. Büttner, A. Romanyuk, P. Oelhafen, *Surf. Sci.* **2005**, *590*, 146.

[8] M. Manolova, M. Kayser, D. M. Kolb, H.-G. Boyen, P. Ziemann, D. Mayer, A. Wirth, *Electrochim. Acta* **2007**, *52*, 2740.
[9] M. Manolova, H. G. Boyen, J. Kucera, A. Gross, A. Romanyuk, P. Oelhafen, V. Ivanova, D. M. Kolb, *Adv. Mater.* **2009**, *21*, 320.
[10] J. Kucera, A. Gross, *Langmuir* **2008**, *24*, 13985.
[11] H. G. Boyen, P. Ziemann, U. Wiedwald, V. Ivanova, D. M. Kolb, S. Sakong, A. Gross, A. Romanyuk, M. Büttner, P. Oelhafen, *Nat. Mater.* **2006**, *5*, 394.
[12] J. J. Yeh, I. Lindau, *At. Data Nucl. Data Tables* **1985**, *32*, 1.
[13] D. Qu, K. Uosaki, *J. Phys. Chem. B* **2006**, *110*, 17570.
[14] T. L. Brower, J. C. Garno, A. Ulman, G. Liu, C. Yan, A. Gölzhäuser, M. Grunze, *Langmuir* **2002**, *18* 6207.
[15] G. Cao, H G. Hong, T. E. Mallouk, *Acc. Chem. Res.* **1992**, *25*.
[16] T. L. Brower, J. C. Garno, A. Ulman, G. Liu, C. Yan, A. Gölzhäuser, M. Grunze, *Langmuir* **2002**, *18*.
[17] O. Shekhah, H. Wang, S. Kowarik, F. Schreiber, M. Paulus, M. Tolan, C. Sternemann, F. Evers, D. Zacher, R. A. Fischer, C. Wöll, *J. Am. Chem. Soc.* **2007**, *129*, 15118.
[18] M. Altman, A. D. Shukla, T. Zubkov, G. Evmenenko, P. Dutta, M. E. van der Boom, *J. Am. Chem. Soc.* **2006**, *128*, 7374.
[19] K. Kanaizuka, R. Haruki, O. Sakata, M. Yoshimoto, Y. Akita, H. Kitagawa, *J. Am. Chem. Soc.* **2008**, *130*, 15778.
[20] O. Shekhah, H. Wang, D. Zacher, R. A. Fischer, C. Wöll, *Angew. Chem.* **2009**, *121*, 5138; *Angew. Chem. Int. Ed.* **2009**, *48*, 5038.
[21] B. Jäger, H. Schürmann, H. U. Müller, H.-J. Himmel, M. Neumann, M. Grunze, C. Wöll, *Z. Phys. Chem.* **1997**, *202*, 263.
[22] D. A. Shirley, *Phys. Rev. B* **1972**, *5*, 4709.
[23] T.-S. Lin, W. J. Partin, G. M. Damminga, T. M. Parrill, W.-J. Lee, Y.-W. Chung, *Surf. Sci.* **1987**, *183*, 113.
[24] W. F. Bergerson, J. A. Mulder, R. P. Hsung, X.-Y. Zhu, *J. Am. Chem. Soc.* **1999**, *121*, 454.
[25] M. P. Seah, W. A. Dench, *Surf. Interface Anal.* **1979**, *1*, 2.
[26] D. R. Penn, *Phys. Rev. B* **1987**, *35*, 482.
[27] P. E. Laibinis, C. D. Bain, G. M. Whitesides, *J. Phys. Chem.* **1991**, *95*, 7017.
[28] G. Kresse, J. Furthmüller, *Phys. Rev. B* **1996**, *54*, 11169.
[29] J. P. Perdew, K. Burke, M. Ernzerhof, *Phys. Rev. Lett.* **1996**, *77*, 3865.
[30] P. E. Blöchl, O. Jepsen, O. K. Andersen, *Phys. Rev. B* **1994**, *49*, 16223.
[31] G. Kresse, D. Joubert, *Phys. Rev. B* **1999**, *59*, 1758.

Communications

Hybrid Composites

F. Eberle, M. Saitner, H.-G. Boyen,*
J. Kucera, A. Gross, A. Romanyuk,
P. Oelhafen, M. D'Olieslaeger,
M. Manolova, D. M. Kolb ____ ▮▮▮▮–▮▮▮▮

A Molecular Double Decker: Extending the Limits of CurrentMetal–Molecule Hybrid Structures

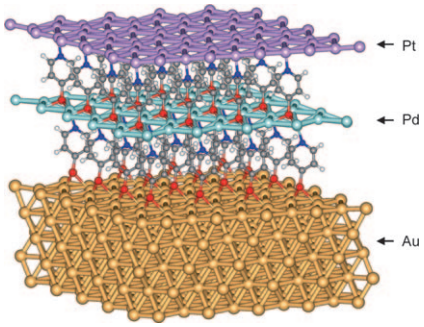

Towards the third dimension: A new type of organic–inorganic hybrid comprises two independent molecular layers separated by a metal monolayer and sandwiched between outer electrodes (see picture). The interlayer reveals metallic properties despite its reduced dimensions and the presence of chemical bonds at both sides. It might be useful as an intermediate electrode to control charge transport through molecule-based devices.